



**HAL**  
open science

## Improvement in the morphology of Ti-based surfaces: a new process to increase in vitro human osteoblast response

Maxence Bigerelle, Karine Anselme, B. Noël, I. Ruderman, Pierre Hardouin, A. Iost

### ► To cite this version:

Maxence Bigerelle, Karine Anselme, B. Noël, I. Ruderman, Pierre Hardouin, et al.. Improvement in the morphology of Ti-based surfaces: a new process to increase in vitro human osteoblast response. *Biomaterials*, 2002, 23 (7), pp.1563-1577. 10.1016/S0142-9612(01)00271-X . hal-04546114

**HAL Id: hal-04546114**

**<https://hal.science/hal-04546114>**

Submitted on 15 Apr 2024

**HAL** is a multi-disciplinary open access archive for the deposit and dissemination of scientific research documents, whether they are published or not. The documents may come from teaching and research institutions in France or abroad, or from public or private research centers.

L'archive ouverte pluridisciplinaire **HAL**, est destinée au dépôt et à la diffusion de documents scientifiques de niveau recherche, publiés ou non, émanant des établissements d'enseignement et de recherche français ou étrangers, des laboratoires publics ou privés.

# Improvement in the morphology of Ti-based surfaces: a new process to increase in vitro human osteoblast response

M. Bigerelle<sup>a,b</sup>, K. Anselme<sup>c,\*</sup>, B. Noël<sup>c</sup>, I. Ruderman<sup>a,b</sup>, P. Hardouin<sup>c</sup>, A. Iost<sup>a,b</sup>

<sup>a</sup> *Equipe "Surfaces et Interfaces" ENSAM Lille, 8 Boulevard Louis XIV, 59046 Lille Cedex, France*

<sup>b</sup> *Laboratoire de Métallurgie Physique et Génie des Matériaux UMR CNRS 8517, 59655 Villeneuve d'Ascq Cedex, France*

<sup>c</sup> *Institut de Recherche sur les Biomatériaux et les Biotechnologies (IR2B), Université du Littoral et de la Côte d'Opale, 52 rue du Dr Calot, 62608 Berck-sur-Mer, France*

---

## Abstract

Surface roughness has been shown to be an influencing parameter for cell response. In this experience we attempted to compare the effect of roughness organization of Ti6Al4V or pure titanium substrates on human osteoblast (hOB) response (proliferation, adhesion). Surface roughness was extensively analyzed at scales above the cell size (macro-roughness) or below the cell size (micro-roughness) by calculation of relevant classic amplitude parameters (Ra, Rt) and original frequency parameters (Order, Delta). We developed a new process to prepare isotropic surfaces (electro-erosion), which were compared to isotropic surfaces obtained by polishing and anisotropic surfaces obtained by machine-tooling. The hOB response on electro-eroded (EE) Ti6Al4V surfaces or pure titanium (Ti) surfaces was largely increased when compared to polished or machine-tooled surfaces after 21 days of culture. Moreover, the polygonal morphology of hOB on these EE surfaces was very close to the aspects of hOB in vivo on human bone trabeculae.

By a complete description of the surface topography of EE surfaces, we concluded that when the topography was considered below the cell scale, hOB appreciated their isotropic smooth aspect, although when the topography was considered above the cell scale they appreciated their rough isotropic 'landscape' formed by many 'bowl-like nests' favouring cell adhesion and growth. Electro-erosion is a promising method for preparation of bone implant surfaces, as it could easily be applied to preparation of most biomaterials with complex geometries.

*Keywords:* Titanium; Surface roughness; Osteoblasts; Electro-erosion; Adhesion; Proliferation

---

## 1. Introduction

The integration of metallic implants into bone is of great interest to research on biomaterials and a great number of studies are carried out to optimise the bone/biomaterials interface. At this time, orthopaedic implants are used more and more (notably because of the increase in the elderly population) but have a relatively low life span in the body so that retrieval and replacement of implants will be increasingly needed. Consequently, improvement of the integration of biomaterials into bone tissue is one of the challenges of the biomaterials field. Classically, to improve bone tissue integration on implant surfaces, various techni-

ques have been used to increase the roughness of the implant surfaces [1–3]. Many in vivo studies have compared the efficiency of various surface treatments in mechanically and morphologically improving bone tissue integration of implants [3–5]. Various results have been obtained, depending on the roughness amplitude but also on the method used to produce the surface roughness [1–4,6].

Cell adhesion is one of the initial events essential to subsequent proliferation and differentiation of bone cells before bone tissue formation. Consequently, many in vitro evaluations of cell adhesion on substrates with various roughnesses have been performed in order to discern the main surface properties influencing the cell response to implant surfaces [7–12]. Cell adhesion is a very specific parameter and describes the relative adherence of a cell to its substrate, generally at an early stage of culture when the cells are directly in contact

---

\*Corresponding author. Tel.: +33-321-892029; fax: +33-321-892070.

*E-mail address:* kanselme@hopale.com (K. Anselme).

with the material surface [13]. In our opinion, it is necessary to evaluate not only adhesion at an early stage of culture but also to evaluate cell adhesion after several days. An *in vitro* evaluation of cell adhesion 12 h after inoculation is not sufficient to anticipate the future integration of a material several weeks after implantation. *In vivo*, the biomaterial integration implies the establishment of a cell/matrix/material interface and the future integration of the implant depends on its solidity. Then, we chose to develop a progressive enzymatic cell detachment method to assess cell adhesion by measuring cell/matrix/substrate bond strength at time points greater than one day and we named it ‘cell/matrix/substrate adhesion’ (CMS adhesion) [14,15].

Using this method, we demonstrated that surface roughness appeared to be an influencing parameter for CMS adhesion but not easily set apart from surface chemistry [16]. Moreover, surface roughness need to be considered not only in term of amplitude but also in terms of organization [14,17]. In previous studies, we quantitatively evaluated the CMS adhesion of hOBs on titanium substrates with various roughness [14]. In addition to currently analyzed roughness magnitude parameters, we defined a fractal dimension parameter representing the roughness organization (Delta). We experimentally showed lower CMS adhesion and proliferation on surfaces with a high Delta, i.e. chaotic surfaces when observed at a scale below the cell size. By modelization of the contact area between a cell and a substrate, we demonstrated that the more the fractal dimension of the substrate increased, the more the contact area between the cell and substrate decreased, meaning that cells adhered less to surfaces presenting too many irregularities because of their inability to establish enough contact area with substrates [14].

In order to thoroughly investigate the influence of roughness organization on osteoblasts, we developed a new study comparing titanium-based substrates treated by various techniques to produce organized (anisotropic) and disorganized (isotropic) surfaces with the same roughness amplitude. Moreover, we attempted to consider the topography at various scales. At the scale above the cell size (macro-roughness) we took into

account the ‘landscape’ around cells and at the scale below the cell size (micro-roughness), we rated the surface with which the ventral membranes of cells have to establish contact. We defined parameters describing organization (frequency) and amplitude of roughness at each scale. To analyse the topography of the substrates below the cell scale, we undertook filtering of original profiles to calculate relevant micro-roughness parameters. These micro-roughness parameters were correlated with cellular parameters (proliferation, CMS adhesion).

## 2. Materials and methods

### 2.1. Surface preparation

To obtain various surface morphologies, titanium alloy Ti6Al4V (A, B, C, D, H, I, MP) and pure titanium (Ti) samples (M, N, O) were machine-tooled under different conditions (anisotropic surfaces (A, B), isotropic surfaces (H)), electro-eroded (EE) (isotropic surfaces (C, D, M, N)) and polished (isotropic surfaces (I, MP, O)). In order to attempt to isolate the effect of surface roughness from that of surface chemistry, some Ti-based and Ti6Al4V-based EE samples were covered with a very thin film of gold–palladium (Au–Pd) that statistically does not affect the numerical values of the roughness parameters (D', I', N', O'). The characteristics of the samples prepared for 3 successive experiments are described in Table 1.

#### 2.1.1. Machine-tooling

Titanium alloy Ti6Al4V bars (14 mm in diameter) were machine-tooled in our laboratory using a classic Cazeneuve HB725 lathe (Groupe CaTo, Pont-Eveque, France) to obtain samples measuring 2 mm in thickness. The conditions for machine-tooling were calculated to obtain grooved surfaces with various roughness amplitudes (Ra) (A, B, H).

To obtain such surfaces, we chose a turning tool with a radius of 1.2 mm. We selected a rotation speed of 2500 rpm. To obtain two different depth and width values for grooves, we selected the radius speed of 0.15 mm/rotation (sample A) and 0.2 mm/rotation

Table 1  
Characteristics of the samples prepared for each experiment

| Ra (μm) | First experiment: Ti6Al4V samples |                |           | Second experiment: titanium samples |           | Third experiment: recovering |    |
|---------|-----------------------------------|----------------|-----------|-------------------------------------|-----------|------------------------------|----|
|         | Electro-erosion                   | Tool machining | Polishing | Electro-erosion                     | Polishing | TA6V                         | Ti |
| 3–3.5   | C                                 | H              |           | M                                   |           |                              |    |
| 1–3     | D                                 | B              |           | N                                   |           | D'                           | N' |
| 0.3–1   |                                   | A              | I         |                                     | O         | I'                           | O' |
| ~0      |                                   |                | MP        |                                     |           |                              |    |

(sample B) that gives groove widths of 150 and 200  $\mu\text{m}$ , respectively for a theoretical Ra of 0.6 and 1.2  $\mu\text{m}$ . At this speed, calculations show that a circular damaged zone of 2.54 mm in diameter will appear in the centre of the samples. To obtain a chaotic machined surface (sample H), the radius speed should be equal to 1 mm/rotation, which will lead, without pulling out of material, to a theoretical Ra of 25  $\mu\text{m}$  and a groove width of 1000  $\mu\text{m}$ .

### 2.1.2. Electro-erosion process

To obtain such a surface, we used a cutting machine (Wire Machine-tooling AGIECUT, Premier Equipment, Altamonte Springs, FL, USA). The 0.25 mm diameter wire was an alloy of Cu Zn (CuZn37) with a traction strength of 900 N/mm<sup>2</sup>. Two process conditions were chosen to obtain two different surface morphologies. The first ones (C, M) were cut at a power of 3 A. The second ones (D, N) were first cut at this same power and then the tooled face was electro-eroded twice more at decreasing powers (1 and 0.25 A, respectively).

### 2.1.3. Polishing

Using a PDMAX 2 automatic polishing machine (Struers S.A.S., Champigny sur Marne, France), samples were polished, using grade 80 silicon carbide paper (I, O) or mirror-polished, successively using grade 80, 120, 500, 1200 and 4000 silicon carbide paper and 3 and 1  $\mu\text{m}$  diamond paste (MP).

### 2.1.4. Covering

Six samples of each type (D, N, I and O) were sputter-coated with gold-palladium using an Emscope SC 500 (Elexience, Paris, France) for scanning electron microscopy preparation.

## 2.2. Roughness measurement

Roughness was measured using a tactile profilometer (Perthen M4PI, Mahr Mesure, Göttingen, Germany). 5 measures were made on 6 samples for a given roughness. For the machine-tooled surfaces, the scanning length was equal to 4 mm to avoid the damaged zone in the centre of the sample. The scan was made perpendicular to the grooves. For other samples, the scanning length was equal to 12 mm and taken randomly on the surface. Profiles were digitized into 8000 points and analyzed on a computer using a personal software. A hundred roughness parameters were computed.

They could be classified into 2 categories: the amplitude parameters that represent a vertical measure of the roughness (depth of the grooves) and the frequency parameters that represent a horizontal measure of the roughness (width of the grooves).

### Amplitude parameters:

- Ra: Average roughness. This value represents the mean height of the roughness ( $\mu\text{m}$ ).
- Rt: The range of the roughness (maximum height—minimum height) ( $\mu\text{m}$ ).
- Rz<sub>1</sub>...Rz<sub>5</sub>: The profile is divided into five identical parts. For each part, the local Rt (range amplitude Rz<sub>i</sub>) is calculated. The more homogenous the roughness, the nearer the Rz values ( $\mu\text{m}$ ).
- Rz: The Rz<sub>1</sub> to Rz<sub>5</sub> average ( $\mu\text{m}$ ).

### Frequency parameters:

- SM: Mean spacing of the profile irregularities ( $\mu\text{m}$ ).
- Peak: Number of peaks per inch of the profile.
- Autocorrelation parameter: First, we defined a normalized autocorrelation function and found the integer  $i$  as in  $R(i) = 1/Rq^2(N-i) \sum_{j=1}^{N-i} y_j y_{j+i}$  where  $y_i$  are equidistant discontinuous points in  $N$  points and Rq is the well known standard deviation of the amplitude.
  - LAC: Autocorrelation length  $L$  as in  $L = x_{i+1} = 1/e$ .
  - PAS: If the autocorrelation function is periodic, we calculated the period (PAS). PAS represents the width of the periodic grooves ( $\mu\text{m}$ ).
- Order: describes the periodicity of a profile. Order is evaluated on a scale wider than the cell itself.

Supposing a correlation integral  $J$  as in  $J = \int_{x=0}^{x=L} R(x) dx$  representing a sort of fundamental with regard to a function symbolizing a certain order power. We defined the  $K$  series  $I_k$  of integrals  $I_k = \int_{x=kL}^{x=(k+1)L} |R(x)| dx$  that represents a kind of successive harmonics of the order power of profiles. Finally, the order parameter is defined as  $\text{order} = 100 \sum_{i=1}^K I_k / (KJ)$  and lies between 0 (white noise profiles) and 100 (perfect periodic profiles without noise).

- Delta ( $\Delta$ ) is a fractal dimension parameter describing the “derivability” of a profile. The fractal dimension of a profile is comprised between 1 and 2. When the surface is very ordered  $\Delta = 1$  and when the surface is chaotic  $\Delta = 2$ . Delta describes the surface organization at a scale inferior to the width of the cells (from 0.05  $\mu\text{m}$  to 7  $\mu\text{m}$ ).

At first, no filtering was undertaken and the original roughness profiles obtained were considered as describing the “macro-roughness”. To take into account roughness below the cell scale, we filtered the original roughness profiles using a high pass filter. We used the Fourier Transform and retained only those frequencies greater than the inverse of the size of one cell (1/50  $\mu\text{m}$ ). By the inverse Fourier transform, we obtained a new profile from which we calculated new micro-roughness parameters.

Statistical analysis of the micro-roughness effects on cell proliferation and CMS adhesion was performed using SAS<sup>©</sup> software (SAS Institute, Cary, NC).

### 2.3. X-ray diffraction analysis

X-ray diffraction data was obtained in a Siemens DC5000 diffractometer (Bruker AXS GmbH, Karlsruhe, Germany) equipped with a monochromatic Cu K<sub>α</sub> X-ray source. This analysis was carried out on EE samples and polished ones to detect the effects of electro-erosion treatment on Ti6Al4V and Ti notably on oxide layers.

### 2.4. Cell culture

Human osteoblasts were obtained from trabecular bone taken from the iliac crest of young patients. Cells were initially cultured in Dulbecco Modified Essential Medium (DMEM, Eurobio, France) containing 10% fetal bovine serum, 100 units/ml of penicillin, and 100 µg/ml of streptomycin, until confluence and were then preserved in liquid nitrogen in complete DMEM + 10% dimethylsulfoxide (Sigma, L'Isle d'Abeau, France) for several months. The cells were then thawed and cultured in 75 cm<sup>2</sup> flasks. At confluence, the cells were harvested using trypsin-EDTA and inoculated onto samples in 24-well plates for two successive proliferation and CMS adhesion tests. The medium was changed twice a week.

### 2.5. Scanning electron microscopy

Before culture, samples were sputter-coated (Emscope SC 500, Elexience, Paris, France) and examined using a Hitachi S520 scanning electron microscope at an accelerating voltage of 25 kV (Elexience, Paris, France).

Cell layers were fixed in 2% paraformaldehyde (w/v) in monosodic dipotassic 0.2 M buffer, rinsed, dehydrated in graded alcohol, critical-point dried with CO<sub>2</sub> (Emscope CPD 750, Elexience, Paris, France), sputter-coated (Emscope SC 500, Elexience, Paris, France) and examined using a Hitachi S520 scanning electron microscope at an accelerating voltage of 25 kV (Elexience, Paris, France).

### 2.6. Quantitative cell/matrix/substrate (CMS) adhesion test

Samples of each surface were inoculated with 2 to 4 × 10<sup>4</sup> cells/sample. Three samples were analyzed after each incubation period: 24 h, 7 days, 14 days and 21 days. The cells were enzymatically detached from the samples by a diluted trypsin-EDTA (0.025% v/v) treatment as previously described [14]. The percentage

curve of released cells versus trypsination time was established. Area included between the curve and the X-axis was evaluated. The areas obtained were considered as a detachment index (DI) inversely proportional to the CMS adhesion on biomaterial. In some cases, the DI obtained on each surface was divided by the DI on control surface, i.e. Thermanox<sup>®</sup> cell culture treated plastic coverslips (Nunc<sup>™</sup>, Fisher Scientific, Elancourt, France), to calculate the detachment index percentage (DIP).

The experiences were reproduced twice and the results were expressed as the DI average of six samples (three/experiment).

The proliferation curves of human osteoblasts were established from the total detached cell count obtained during the CMS adhesion test after each incubation period.

### 2.7. Modelization of cell proliferation

To determine the relation existing between roughness parameters and cell proliferation, firstly we determined an appropriate statistical model of cell proliferation versus time in culture. The following equation is the best for modelling cell proliferation:

$$P = a \exp(bt) \quad (1)$$

$P$  being the proliferation in function of time, we calculated the proliferation speed  $ab$ :

$$\partial P / \partial t = ab \exp(bt). \quad (2)$$

The regression of Rz values with  $ab$  values give the following equation:

$$ab = 0.069_{\pm 0.003} + 0.037_{\pm 0.005} \log_{10} Rz \quad (3)$$

with a regression coefficient of  $R = 0.95$ .

According to Eq. (2),  $ab$  represents the slope of the curve and is function of culture time ( $t$ ). However, by taking origin ( $t$  near 0), Eq. (2) becomes  $dP/dt = ab$  that is the proliferation rate at the beginning of culture.

### 2.8. Modelization of CMS adhesion

We proceeded, as previously described [14], to the modelization of the DIP with the duration of culture for a given roughness. We chose the following equation:

$$A(t) = \frac{\alpha_0}{1 + \exp(\alpha_1(t - t_0) - \alpha_2)} \quad (4)$$

where  $A(t)$  is the DIP. Thereafter, we introduced a roughness parameter to the equation.

As for proliferation, Rz was chosen:

$$A(t) = \frac{\beta_1}{1 + \exp(\beta_2(t - t_0) + \beta_4(t - t_0)Rz - \beta_3)} \quad (5)$$

By non-linear regression (Newton algorithm), we found:

$$\beta_1 = 107.6_{\pm 6} \quad \beta_2 = 0.0851_{\pm 0.02} \quad \beta_4 = 0.0105_{\pm 0.001} \quad \text{and} \\ \beta_3 = 2.53_{\pm 0.5}$$

with a regression coefficient of  $R = 0.97571$ .

All the coefficients are highly significant which meant that this model was apt to describe CMS adhesion.

$\beta_1$  represents the mean response of tested samples compared to control at the outset.

$\beta_2$  represents the CMS adhesion speed on an ideal smooth surface.

$\beta_3$  represents the length of the initial attachment. The lower  $\beta_3$ , the faster the initial attachment.

$\beta_4$  represents the effect of micro-roughness amplitude (Rz).

An analysis of residue confirmed the relevance of this model (data not shown).

### 3. Results

#### 3.1. Comparison of surfaces treatments on Ti6Al4V samples

##### 3.1.1. Topographical description of surfaces before culture

**3.1.1.1. Surface morphology.** SEM observation of Ti6Al4V machine-tooled surfaces before culture shows circular grooves on A and B surfaces with 150 and 204  $\mu\text{m}$  widths respectively (Fig. 1a,b). To the contrary, H surfaces show irregularly spaced circular large grooves containing many residual smaller grooves with no particular orientation (Fig. 1c). On P80 polished samples (I), many residual grooves with no orientation and with various widths are observed (Fig. 1d). Mirror-polished surfaces are completely smooth (Fig. 1e). No morphological differences are visible between fine and coarse EE surfaces. They are rough and seem to be covered by sheets with the smooth edges associated with some globules (Fig. 1f-h). The surface looks like the result of fusion.

**3.1.1.2. Macro-roughness profiles.** The original profiles confirm the SEM observations. Profiles of A and B machine-tooled surfaces obtain the same regular and periodic morphologies (Fig. 2). The space between grooves is 151  $\mu\text{m}$  for A samples and 205  $\mu\text{m}$  for the B samples. Rz is greater on B samples than on A samples (Table 2). Rz is greater on machine-tooled H samples compared to A and B samples (Table 2). H Samples have a more irregular surface. The H sample profiles contain two components: periodic and stochastic (Fig. 2).

The Rz of polished surfaces (I, MP, O) is low and very homogenous because of low dispersion of the

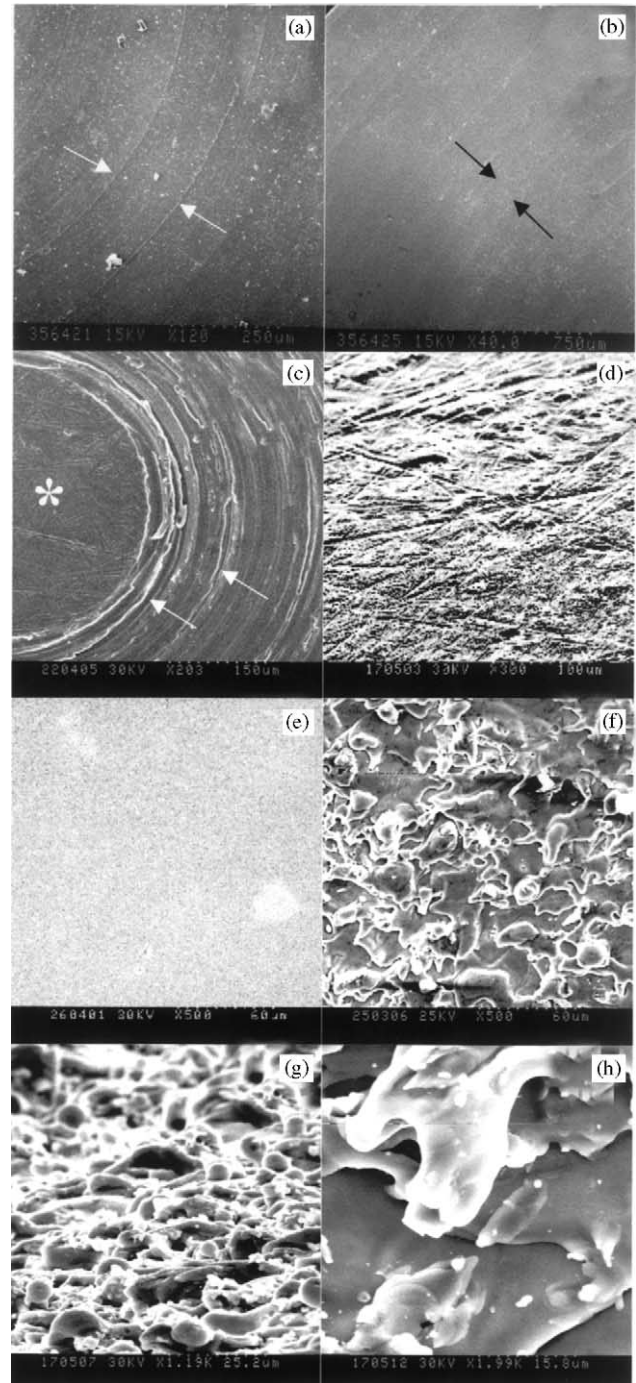


Fig. 1. SEM aspect of surfaces before culture. (a) Machine-tooled Ti6Al4V surface (A). The width of grooves (distance between arrows) is 150  $\mu\text{m}$ . (b) Machine-tooled Ti6Al4V surface (B). The width of grooves (distance between arrows) is 204  $\mu\text{m}$ . (c) Machine-tooled Ti6Al4V surface (H). Irregular grooves (arrows) surround a central polished zone (asterisk). (d) P80 polished titanium surface (O). (e) Mirror-polished Ti6Al4V surface (MP). (f) Fine electro-eroded Ti6Al4V surface (D). (g) Coarse electro-eroded titanium surface (M). (h) Fine electro-eroded titanium surface (N).

Rz<sub>i</sub> values (Table 2). The autocorrelation function presents no periodic component and the order is low, meaning that the polished surfaces are smooth isotropic surfaces (Fig. 2). As for polished surfaces,

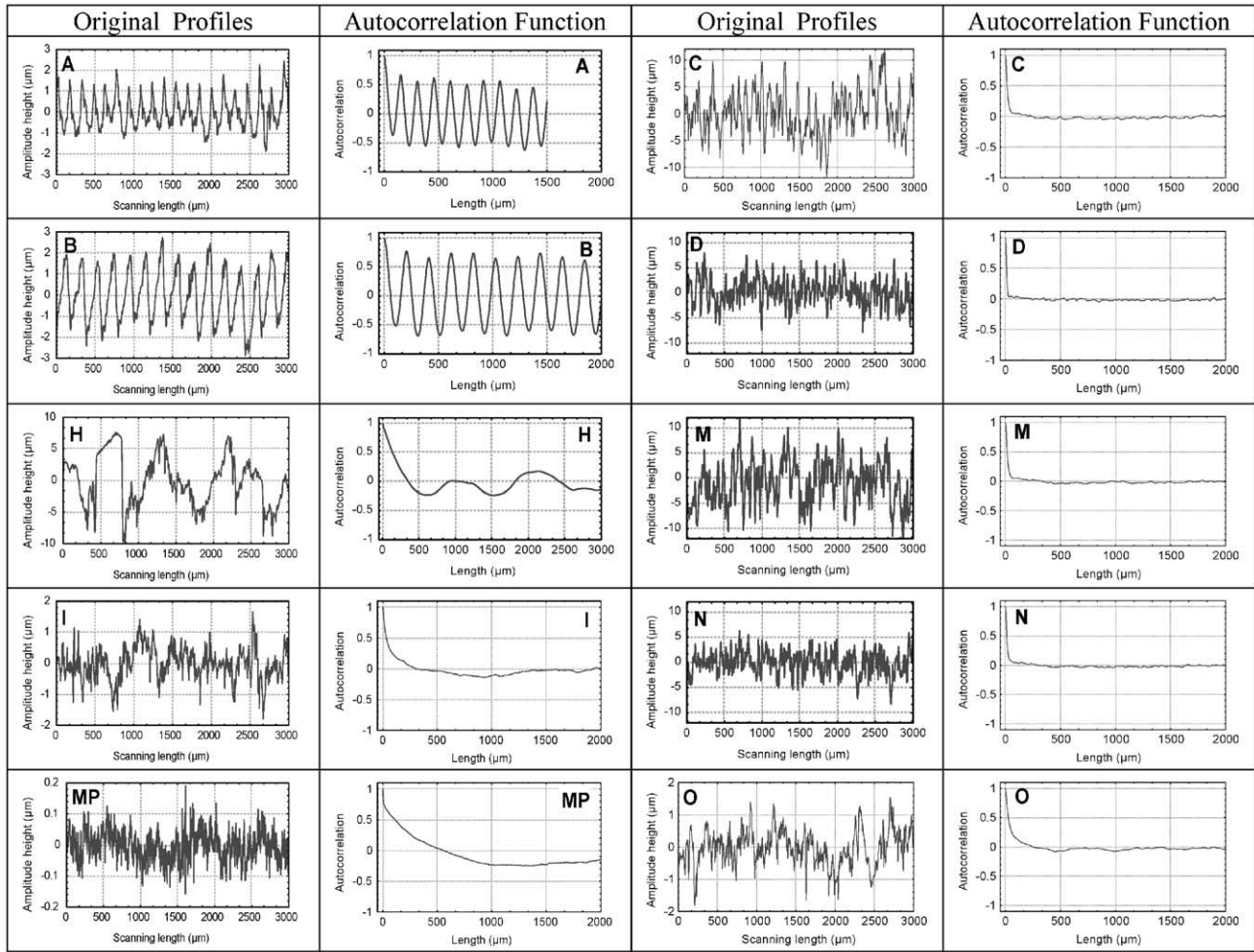


Fig. 2. Macro-roughness original profiles and autocorrelation function profiles for each surface.

Table 2  
Macro-roughness parameters of samples

|    | Ra   | Rt    | Rz <sub>1</sub> | Rz <sub>2</sub> | Rz <sub>3</sub> | Rz <sub>4</sub> | Rz <sub>5</sub> | Rz    | LAC  | Order | Peak | SM   | Delta |
|----|------|-------|-----------------|-----------------|-----------------|-----------------|-----------------|-------|------|-------|------|------|-------|
| A  | 0.8  | 5.23  | 4.06            | 3.90            | 3.99            | 3.76            | 4.14            | 3.97  | 33   | 47    | 194  | 68   | 1.346 |
| B  | 1.21 | 6.53  | 5.27            | 5.18            | 5.23            | 5.33            | 5.48            | 5.30  | 41   | 59    | 146  | 165  | 1.334 |
| H  | 3.35 | 22.2  | 15.7            | 14.22           | 14.04           | 13.40           | 17.41           | 14.96 | 211  | 27    | 138  | 183  | 1.318 |
| MP | 0.07 | 0.73  | 0.44            | 0.44            | 0.46            | 0.46            | 0.45            | 0.45  | 192  | 36    | 1025 | 26   | 1.429 |
| C  | 3.29 | 23.35 | 18.8            | 19.5            | 19.8            | 19.1            | 18.5            | 19.1  | 20.1 | 10.9  | 462  | 54   | 1.145 |
| D  | 2.22 | 15.8  | 13.3            | 13.1            | 13.7            | 13.0            | 13.2            | 13.3  | 12.6 | 8.7   | 598  | 41.9 | 1.157 |
| I  | 0.31 | 3     | 2               | 2               | 2.11            | 1.90            | 2.17            | 1.99  | 63   | 22    | 451  | 58.3 | 1.227 |
| M  | 3.5  | 24.6  | 20.3            | 19.9            | 20.4            | 20.2            | 20.0            | 20.16 | 20.4 | 11.3  | 457  | 54.8 | 1.191 |
| N  | 3.0  | 20.3  | 16.9            | 16.6            | 16.7            | 16.7            | 16.6            | 16.7  | 17.4 | 10.0  | 539  | 50.8 | 1.196 |
| O  | 0.5  | 4.15  | 3.0             | 3.0             | 3.0             | 3.07            | 3.20            | 3.1   | 43.6 | 17.5  | 496  | 50.7 | 1.281 |

the profiles of EE surfaces (C,D,M,N) are quite homogenous because  $Rz_i$  are very close. However, the  $Rz$  values of EE surfaces are largely higher (Table 2). As the order value for EE surfaces is very low ( $\sim 10\%$ ) we consider that EE surfaces are rough isotropic surfaces.

*3.1.1.3. Micro-roughness profiles.* When micro-roughness is taken into account, the  $Rz$  of A and B machine-tooled surfaces lies around  $1.5\mu\text{m}$ , similar to P80 polished surfaces (Table 3). On the contrary, the  $Rz$  of H surfaces remains higher ( $\sim 4\mu\text{m}$ ). Although spacing between micro-grooves (SM) is identical for A,

Table 3  
Micro-roughness parameters of samples (after high-pass filter with cut off 50  $\mu\text{m}$ )

|    | Ra    | Rt    | Rz <sub>1</sub> | Rz <sub>2</sub> | Rz <sub>3</sub> | Rz <sub>4</sub> | Rz <sub>5</sub> | Rz   | LAC  | Order | Peak | SM    | Delta |
|----|-------|-------|-----------------|-----------------|-----------------|-----------------|-----------------|------|------|-------|------|-------|-------|
| A  | 0.15  | 1.87  | 1.39            | 1.01            | 0.99            | 1.12            | 1.45            | 1.19 | 6.02 | 23.4  | 1207 | 20.9  | 1.460 |
| B  | 0.15  | 4.49  | 2.89            | 1.05            | 1.06            | 1.11            | 2.85            | 1.79 | 6.05 | 15.2  | 1084 | 23.2  | 1.471 |
| H  | 0.37  | 6.30  | 4.71            | 3.69            | 3.96            | 3.42            | 4.89            | 4.13 | 5.95 | 9.60  | 1145 | 21.9  | 1.437 |
| MP | 0.03  | 0.66  | 0.34            | 0.28            | 0.34            | 0.43            | 0.49            | 0.37 | 6.61 | 6.80  | 2049 | 12.1  | 1.491 |
| C  | 1.35  | 11.51 | 9.97            | 9.65            | 9.57            | 9.46            | 9.37            | 9.61 | 6.05 | 9.52  | 955  | 26.4  | 1.228 |
| D  | 1.23  | 10.17 | 8.43            | 8.50            | 8.74            | 8.70            | 8.64            | 8.60 | 5.95 | 9.78  | 966  | 26.1  | 1.251 |
| I  | 0.18  | 2.11  | 1.69            | 1.45            | 1.61            | 1.67            | 1.68            | 1.62 | 13.5 | 12.2  | 726  | 35.1  | 1.284 |
| M  | 1.42  | 11.87 | 10.29           | 9.97            | 9.72            | 9.65            | 10.19           | 9.96 | 6.19 | 10.29 | 949  | 26.5  | 1.309 |
| N  | 1.25  | 11.33 | 9.41            | 8.68            | 8.91            | 8.90            | 8.94            | 8.97 | 6.26 | 10.15 | 981  | 25.9  | 1.331 |
| O  | 0.165 | 2.15  | 1.64            | 1.46            | 1.48            | 1.45            | 1.63            | 1.53 | 5.02 | 8.15  | 1356 | 18.62 | 1.387 |

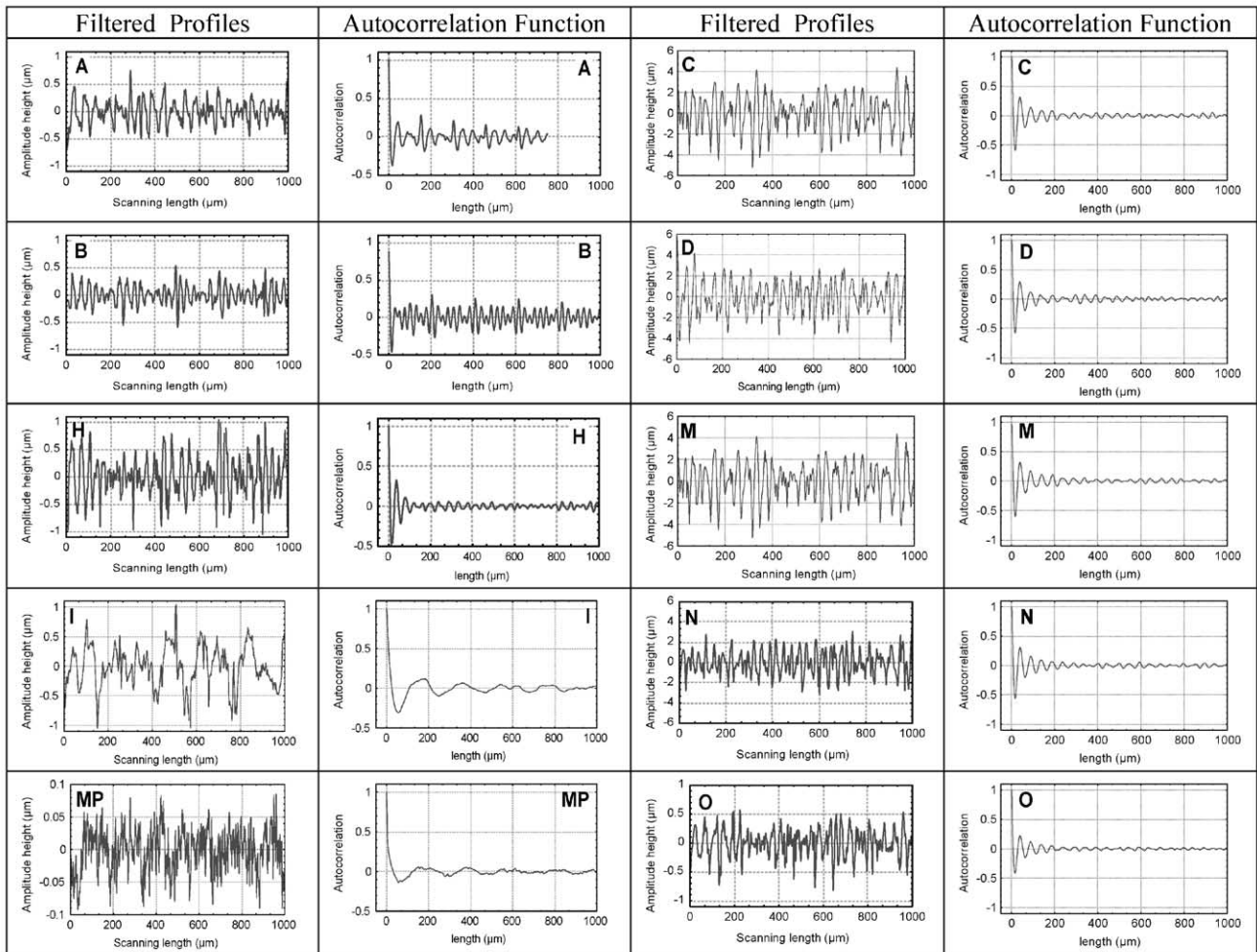


Fig. 3. Micro-roughness profiles obtained after filtering and autocorrelation function profiles for each surface.

B and H surfaces, the autocorrelation function demonstrates the periodic aspect of A and B profiles and the un-periodic aspect of the H profile (Fig. 3). This is confirmed by the values of the order parameter:  $B > A > H$  (Table 3). Machine-tooled surfaces are anisotropic surfaces with (A, B) or without periodicity (H).

As at the macro-roughness level, the  $Rz_i$  values for EE surfaces (C, D, M, N) are very stable (Table 3). The profiles of EE surfaces are very homogenous (Fig. 3). The fine EE surfaces (D, N) have the same frequency parameters as coarse EE surfaces (C, M) but lower amplitude parameters (Table 3).

The comparison of autocorrelation functions between the 2 types of isotropic surfaces (EE and polished surfaces) shows that EE surfaces are more homogeneous at each level of observation (macro- and micro-roughness) than polished ones (Fig. 3). The polished Ti6Al4V-based surfaces (I) have a quite irregular micro-roughness compared to polished Ti-based surfaces (O) (Fig. 3).

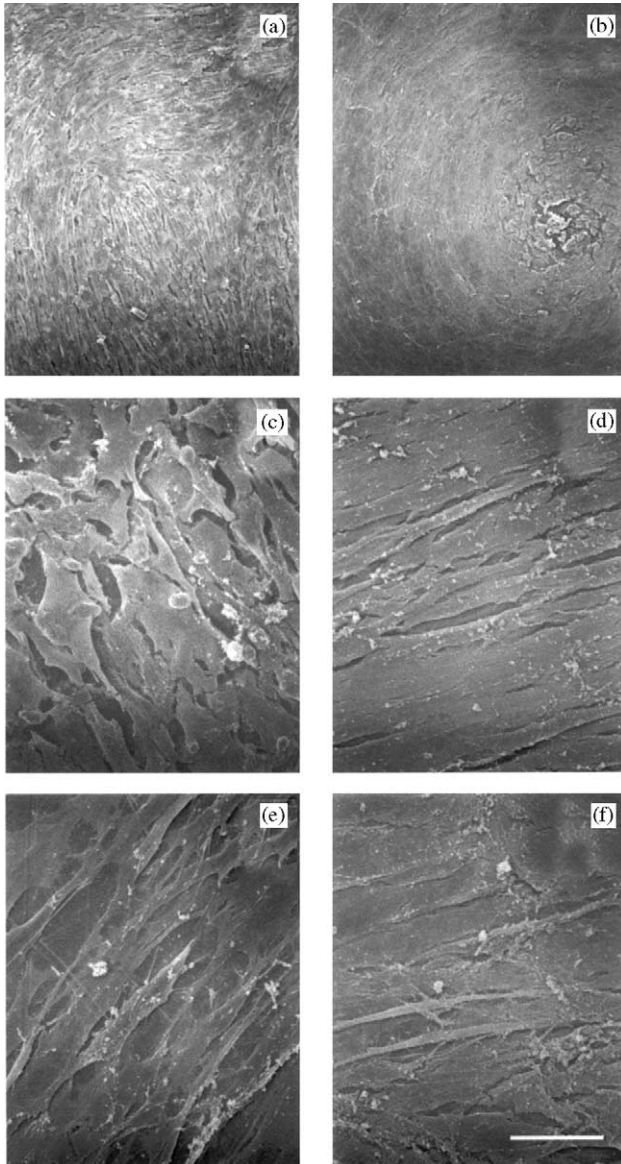


Fig. 4. SEM observation of cells. (a) Cells cultured during 7 days on (D) electro-eroded surfaces (bar = 100  $\mu\text{m}$ ). (b) Cells cultured during 7 days on (B) machine-tooled surfaces (bar = 250  $\mu\text{m}$ ). (c) Cells cultured during 7 days on (D) electro-eroded surfaces (bar = 20  $\mu\text{m}$ ). (d) Cells cultured during 7 days on (B) machine-tooled surfaces (bar = 20  $\mu\text{m}$ ). (e) Cells cultured during 7 days on (I) P80 polished surfaces (bar = 20  $\mu\text{m}$ ). (f) Cells cultured during 7 days on (MP) mirror-polished surfaces (bar = 20  $\mu\text{m}$ ).

### 3.1.2. Cell morphology

At the beginning of culture, cells on all surfaces are relatively separated from each other and display a polygonal morphology (not shown). After 7 days, the morphology of cells cultured on the various surfaces becomes widely different. Observation of the cell layer at low magnification after 7 days of culture shows that no specific organization was visible on EE surfaces (Fig. 4a) although the organization of the cell layer follows the grooves produced by machine-tooling (Fig. 4b). Moreover, the cell morphology on polished and machine-tooled surfaces was really different from the cell morphology on EE surfaces. Cells on EE surfaces showed a very polygonal aspect with no cell extensions (Fig. 4c) although on machine-tooled (Fig. 4d) and polished (Figs. 4e,f) surfaces, cells were very fusiform with many filamentous extensions and oriented in a parallel manner. After 14 and 21 days, cells are confluent and an extracellular matrix can be seen in some cases under a cell monolayer (not shown).

### 3.1.3. Effect of roughness on cell proliferation

The comparison of osteoblast proliferation on these various surfaces shows some differences (Fig. 5). EE surfaces are more favourable to osteoblast proliferation than polished or machine-tooled surfaces. However, we can observe that cell proliferation on a coarse and irregular machine-tooled surface (H) is closer to proliferation on EE surfaces (C and D) than on controlled and regular machine-tooled surfaces (A and B).

Concerning the proliferation speed  $ab$ , it increases with  $Rz$  but a plateau is attained for high values of  $Rz$  (Fig. 6).

### 3.1.4. Effect of roughness on CMS adhesion

The human osteoblast detachment index (DI) decreases, i.e. CMS adhesion increases, on all surfaces compared to control surface (Thermanox<sup>®</sup>) as a function of time (Fig. 7) notably after 14 and 21 days of culture. When comparing the various surfaces, only DI on coarse EE surfaces (C) is lower than on control surface after 1 and 7 days of culture. After 14 days of culture, only DI on EE surfaces (C, D) are significantly lower than on control. After 21 days, DI on all surfaces except MP ones are significantly lower than on control. At that point, the CMS adhesion on EE surfaces is very much higher than on machine-tooled or polished surfaces.

By modelization of the DIP with the duration of culture and roughness amplitude ( $Rz$ ) we established the Fig. 8. This model confirms that the DIP decreases with time notably on surfaces with high roughness amplitude.

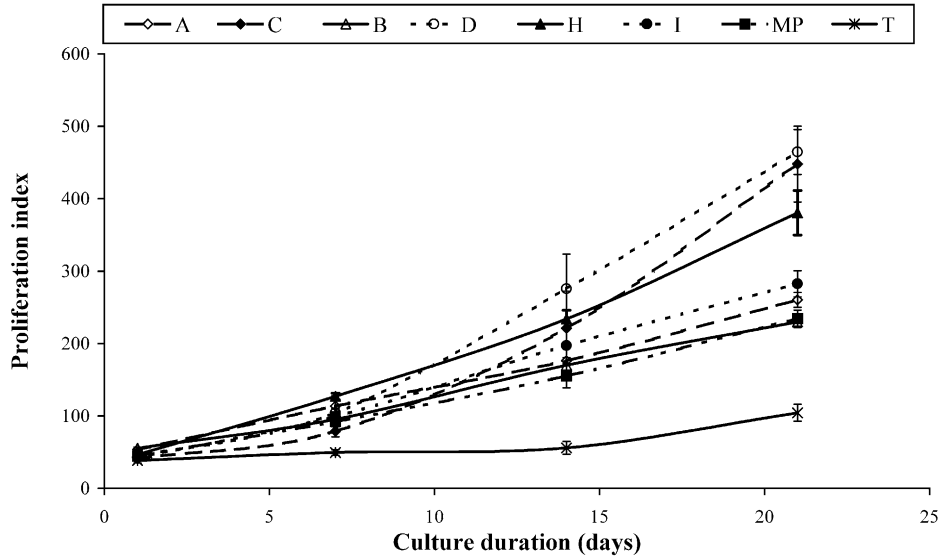


Fig. 5. Proliferation curves on the various tested surfaces as a function of time. (A) Controlled machine-tooled Ti6Al4V surface with 150  $\mu\text{m}$  grooves. (C) Coarse electro-eroded Ti6Al4V surface. (B) Controlled machine-tooled Ti6Al4V surface with 204  $\mu\text{m}$  grooves. (D) Fine electro-eroded Ti6Al4V surface. (H) Coarse machine-tooled Ti6Al4V surface. (I) P80 polished Ti6Al4V surface. (MP) Mirror-polished Ti6Al4V surface. (T) Control cell culture treated plastic coverslips Thermanox<sup>®</sup>. Average cell number and standard error are shown ( $n = 6$ ).

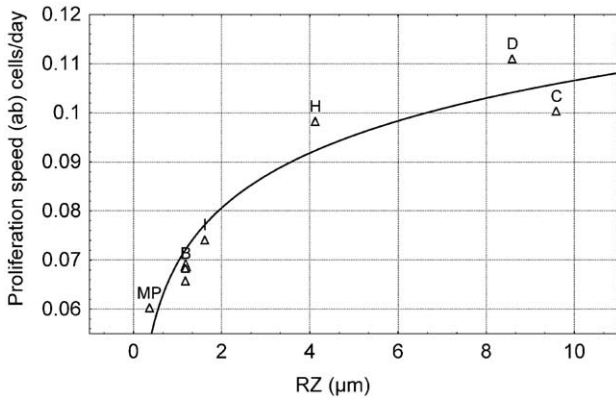


Fig. 6. The proliferation speed  $ab$  (cells/day) obtained from the equation (3) is plotted as a function of  $Rz$  ( $\mu\text{m}$ ).  $ab$  represents the proliferation rate at the beginning of culture. It increases with  $Rz$  but a plateau is attained for high values of  $Rz$ .

### 3.2. Comparison of electro-eroded Ti6Al4V and Ti samples

As the very good cell response we obtained on EE surfaces may be related to surface chemistry transformation on the Ti6Al4V alloy, we developed further experiments to thoroughly examine the effects of the electro-erosion process on the surface topography and chemistry of pure titanium compared to Ti6Al4V alloy.

There are no morphological differences between the fine and coarse EE surfaces on Ti6Al4V (C, D) and Ti samples (M, N) (Fig. 1f,g). The P80 polished Ti surfaces (O) have the same aspect as P80 polished Ti6Al4V surfaces (I) (Fig. 1d).

When CMS adhesion is compared on Ti6Al4V and Ti EE and polished samples, the DI decreases as a function of time, particularly on EE surfaces (Fig. 9). After 1 day, there is no significant difference of DI on the different surfaces. After 7 days of culture, CMS adhesion is only significantly higher on coarse Ti-based EE surfaces (M). When comparing the various surfaces after 14 and 21 days, DI on EE surfaces is significantly lower than on the control surfaces, whatever the material used. CMS adhesion is the same on Ti-based or Ti6Al4V-based EE surfaces.

The morphology of cells on Ti-based and Ti6Al4V-based EE surfaces is the same (Figs. 10a,b). Cells have a very intimate contact with surfaces. They are very difficult to distinguish from the surface. They look like they are part of the surface roughness (Figs. 10c,d).

### 3.3. Chemical description of surfaces

In order to analyse the oxide layer on our samples, we undertook an X-ray diffraction analysis. Spectra were obtained from the Ti and Ti6Al4V samples for electro-erosion and the polishing process. The electro-erosion process may be at the origin of an oxide formation since the metal was cut by melting and cooled under pure water. On X-ray diffraction spectra, a peak was located for both Ti and Ti6Al4V at  $50^\circ$  that characterized the  $\text{TiO}_2$  oxide layer (Fig. 11). Some very small peaks corresponding to others oxides ( $\text{TiO}$ ,  $\text{Ti}_3\text{O}_5$ ,  $\text{Ti}_6\text{O}_{11}$ , and  $\text{Ti}_5\text{O}_9$ ) were also observed (not shown). Finally, the heat treatment during EE process trans-

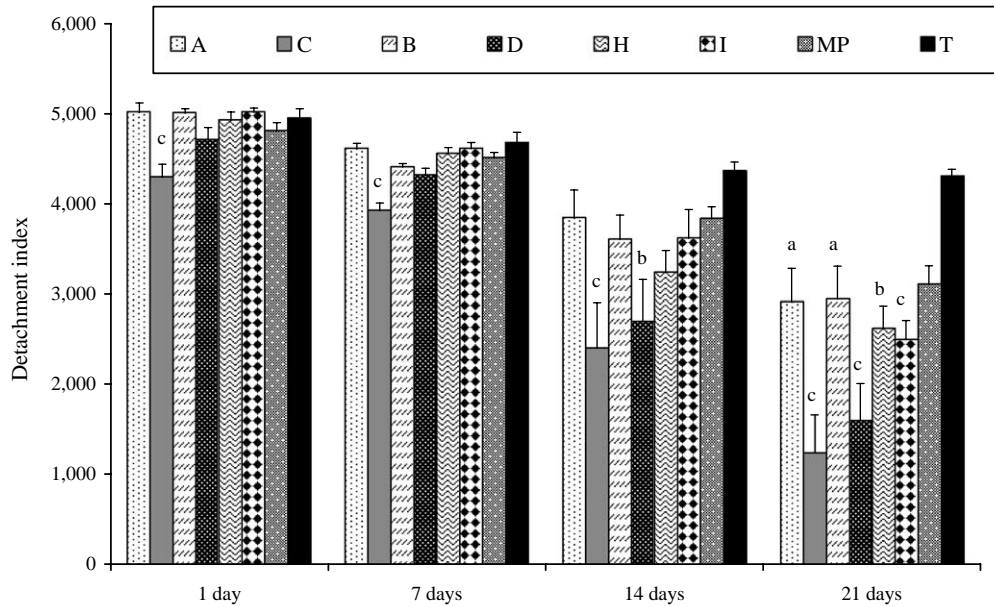


Fig. 7. Time course of detachment index (DI) of cells cultured on Ti6Al4V substrates with various surface organization. (A) Controlled machine-tooled surface with 150  $\mu\text{m}$  grooves. (C) Coarse electro-eroded surface. (B) Controlled machine-tooled surface with 204  $\mu\text{m}$  grooves. (D) Fine electro-eroded surface. (H) Coarse machine-tooled surface. (I) P80 polished surface. (MP) Mirror-polished surface. (T) Control cell culture treated plastic coverslips Thermanox<sup>®</sup>. The DI decreases, i.e. CMS adhesion increases, on all surfaces as a function of time. Data indicate the mean + standard error ( $n = 6$ ). a—significantly different from Thermanox<sup>®</sup> at  $p \leq 0.05$ . b—significantly different from Thermanox<sup>®</sup> at  $p \leq 0.01$ . c—significantly different from Thermanox<sup>®</sup> at  $p \leq 0.001$ .

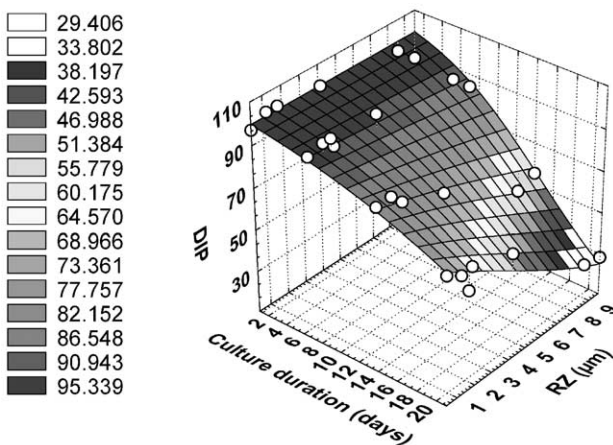


Fig. 8. 3D plot of time course of DIP in function of Rz ( $\mu\text{m}$ ). This plot was drawn from the Eq. (5) obtained after modelization of the DIP with the duration of culture for a given roughness. This model correlates with experimental values with a regression coefficient of  $R = 0.97571$  and confirms that DIP decreases with time and with roughness amplitude.

formed the surface to a thin film of titanium oxide (mainly  $\text{TiO}_2$ ) that was not detected on the polished surfaces.

### 3.4. Covering of electro-eroded surfaces

Because of the presence of this titanium oxide layer on the EE surfaces, we can not conclude on the relative influence of surface morphology or surface chemistry on

the CMS adhesion to these surfaces. In order to attempt to isolate the effect of surface roughness from that of surface chemistry, we covered Ti-based and Ti6Al4V-based EE surfaces with a very thin film of gold-palladium that statistically did not affect the numerical values of the order parameters.

After 21 days of culture, DI was not modified by the covering of surfaces except on Ti-based EE surfaces (N) and Ti-based polished surfaces (O) where covering induced a significant decrease in DI i.e. an increase of CMS adhesion (Fig. 12).

## 4. Discussion

Our quantitative CSM adhesion test demonstrated major differences of cell detachment in function of surface roughness and particularly at later delays (14 and 21 days). Just after inoculation cells adhere directly on the surface of the material (cell/material interface) and later on a layer of extracellular matrix proteins (cell/extracellular matrix/material interface). Thus, our measure corresponds early to the detachment of cells from materials and later from the protein layer. Finally, the CSM adhesion parameter appreciates the quality of the cell/material interface. A lower detachment after several days means that the interface is evolved and is more closed to the *in vivo* cell/matrix/material interface.

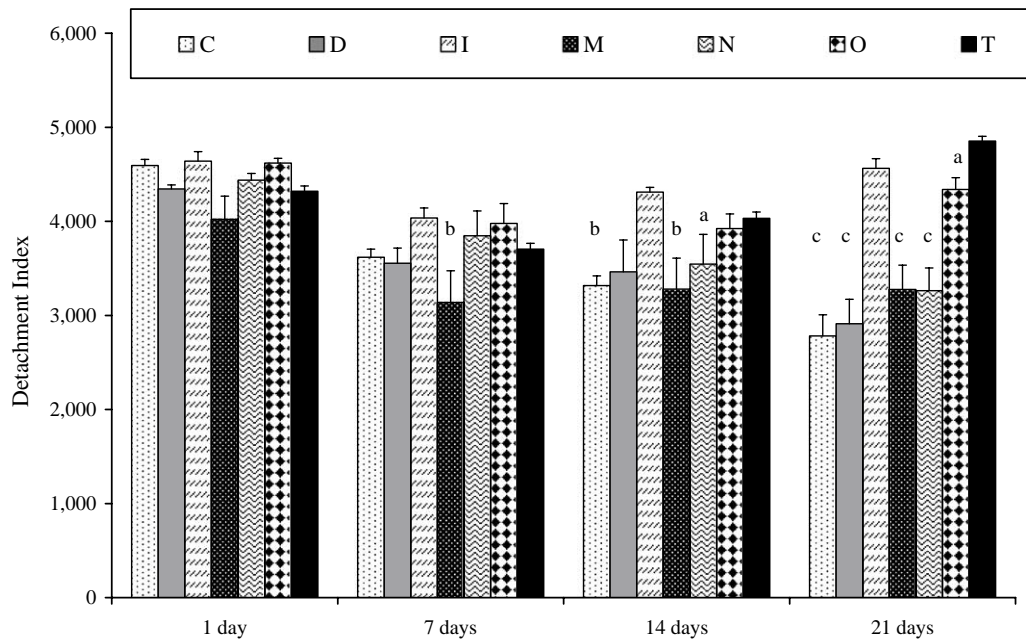


Fig. 9. Time course of detachment index (DI) of cells cultured on electro-eroded Ti6Al4V and titanium surfaces compared to polished surfaces. (C) Coarse electro-eroded Ti6Al4V surface, (D) fine electro-eroded Ti6Al4V surface, (I) polished Ti6Al4V surface, (M) coarse electro-eroded titanium surface, (N) fine electro-eroded titanium surface, (O) polished titanium surface, and (T) Thermanox<sup>®</sup> cell culture treated plastic coverslips. The DI decreases, i.e. CMS adhesion increases, on all surfaces as a function of time. Data indicate the mean + standard error ( $n = 6$ ). a—Significantly different from Thermanox<sup>®</sup> at  $p \leq 0.05$ . b—Significantly different from Thermanox<sup>®</sup> at  $p \leq 0.01$ . c—Significantly different from Thermanox<sup>®</sup> at  $p \leq 0.001$ .

Because covering induced an increase in CMS adhesion on EE and polished titanium surfaces rather than a decrease, diverse hypothesis could be proposed. Either the Au–Pd layer improves the biocompatibility of titanium substrates or the titanium oxide layer formed on titanium substrates has a more negative effect on CMS adhesion than the titanium oxide layer formed on Ti6Al4V substrates. In the first hypothesis, the CMS adhesion would be improved on all recovered surfaces. In the second hypothesis, the oxide layer formed on titanium substrates would be more ‘cytotoxic’ than oxides formed on Ti6Al4V substrates. This is unlikely because the cytocompatibility of titanium is well known [18,19,5] and because we did not observe any difference of CMS adhesion in a direct comparison of EE and polished titanium and Ti6Al4V substrates (Fig. 9). Only a thorough characterization of the surface chemistry of EE samples will allow us to better interpret these results and to better discriminate between the relative quality of the oxide layers on the titanium and Ti6Al4V substrates. These analyses are in progress.

In this paper, we focused on the effect of surface roughness on hOB proliferation and CMS adhesion and especially on the EE surface effects. The high proliferation and CMS adhesion we observed on EE surfaces could be related to the hypothesis of Curtis and Clark who consider that cells react to discontinuities [20]. They have defined discontinuity as a radius of curvature less

than the average length of a pseudopodium or of the distance part of the sensing elements that control movement [21]. Jansen and co-workers observed that on micro-grooved titanium surfaces a minimum  $1 \mu\text{m}$  width of grooves induced fibroblast orientation in vitro although on  $5$  and  $10 \mu\text{m}$  wide grooved surfaces this orientation was not observed [22]. They hypothesized that the phenomenon of contact guidance was the result of a mechanoreceptive response to surface discontinuities implying the dynamics of the cytoskeleton [23]. The front edges of cells, the lamellipodia, contain actin microspikes which could be influenced by surface discontinuities. When a spike faces a ridge it would be faced with an unfavourable force and would not rise to actin polymerization. Consequently, actin filaments would form and elongate, oriented along the groove direction. This process should proceed until the cell on the microgrooved substratum reaches a state of equilibrium. Considering this hypothesis, we assumed that this phenomenon was not only implied in cell orientation but may also be at the origin of the ‘installation’ of a cell in a site favourable to its adhesion and future proliferation and differentiation. Thereafter, we attempted to confront our observations with these hypotheses.

In Table 4 we summarized the response of hOB versus the various types of substrates tested in function of the most significant parameters at the macro- and micro-roughness levels.

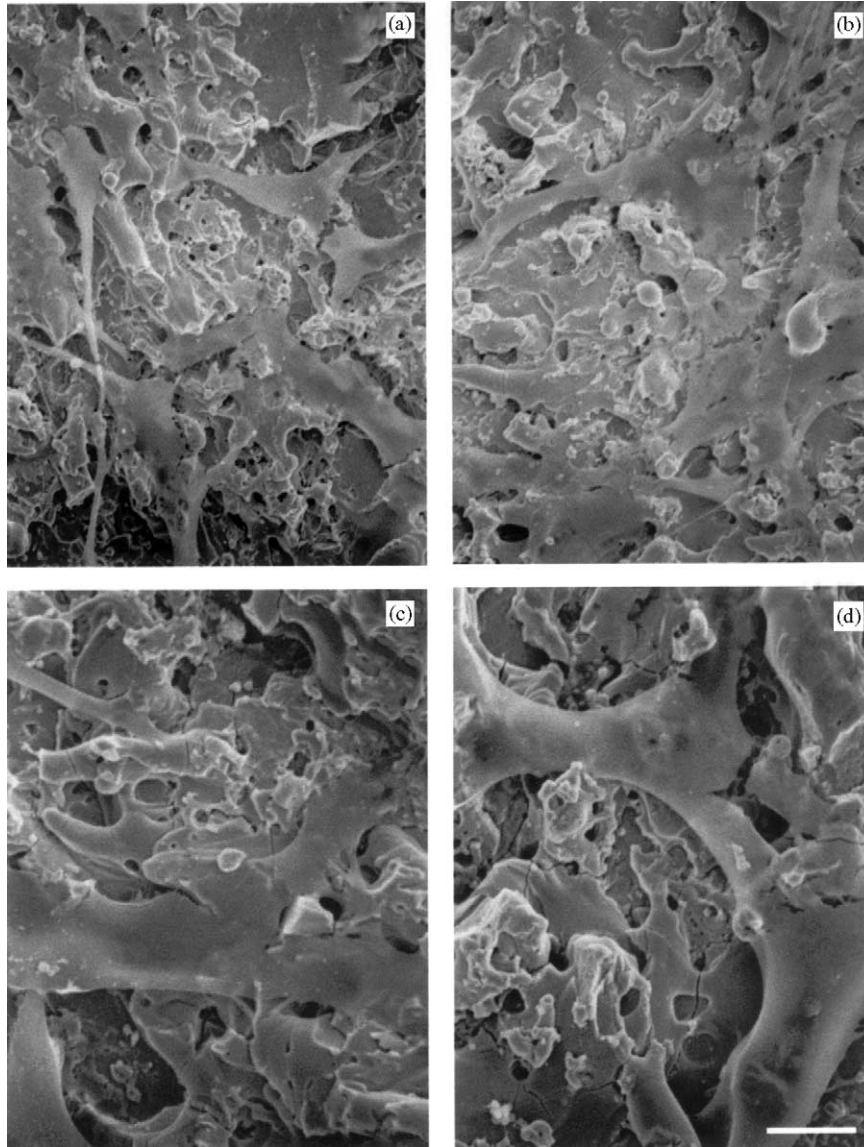


Fig. 10. SEM observation of cells cultured on electro-eroded surfaces. (a) Cells cultured during 7 days on coarse electro-eroded Ti6Al4V surfaces (C) (bar = 20  $\mu\text{m}$ ). (b) Cells cultured during 7 days on coarse electro-eroded titanium surfaces (M) (bar = 20  $\mu\text{m}$ ). (c) Cells cultured during 14 days on coarse electro-eroded Ti6Al4V surfaces (C) (bar = 40  $\mu\text{m}$ ). (d) Cells cultured during 14 days on coarse electro-eroded titanium surfaces (M) (bar = 40  $\mu\text{m}$ ). The morphology of cells on Ti-based and Ti6Al4V-based EE surfaces is the same. Cells have a very intimate contact with surfaces. They are very difficult to distinguish from the surface. They look like they are part of the surface roughness.

From our observations, we can conclude that polished surfaces did not present enough discontinuities or presented discontinuities with a too-low level of amplitude ( $R_z$ ) and/or frequency (Order) to permit cell orientation or to favour adhesion. On the other hand, all grooved surfaces presented discontinuities with minimal characteristics for cell orientation although only coarse grooved surfaces (H) presented discontinuities with a sufficient level of amplitude and frequency to improve adhesion. Thus, it appears that a first threshold exists for discontinuity characteristics enabling cell orientation, which is lower than the second threshold improving adhesion and cell proliferation. The  $R_z$  values would

stay at around 4  $\mu\text{m}$  for the first threshold and around 15  $\mu\text{m}$  for the second (Table 2). However, as the  $R_z$  values for polished surfaces are very close to 4  $\mu\text{m}$  (3.1  $\mu\text{m}$  for O surfaces), it appears more likely that the major factor influencing cell orientation may be organization of the surface roughness which was low on polished surfaces (Order  $\sim$  20) but higher on A and B grooved surfaces (Order = 47 and 59 respectively) than on H coarse grooved surfaces (Order = 27). Once again, this study confirms that organization of the surface topography has a major effect on cell behavior. Comparing H grooved surfaces and EE surfaces to the others, we observe that they present a high roughness

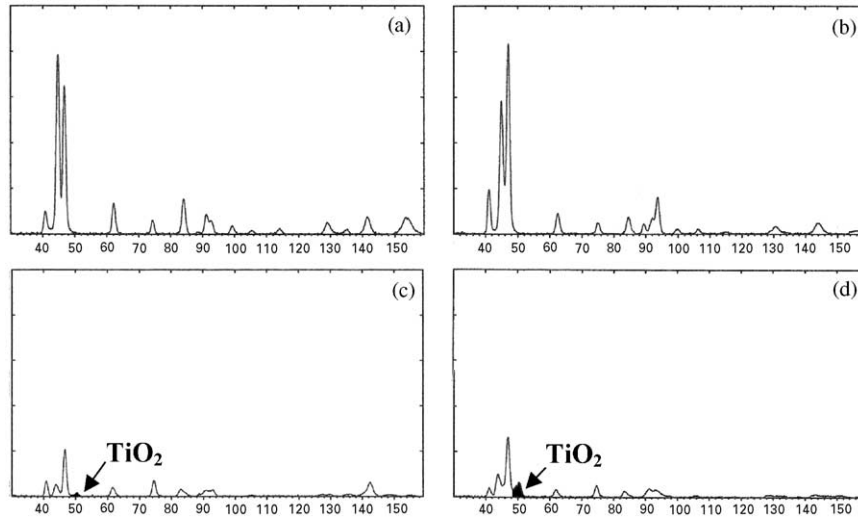


Fig. 11. X-ray diffraction spectra on (a) Polished Ti surface (O). (b) Polished Ti6Al4V surface (I). (c) Fine electro-eroded Ti surface (N). (d) Fine electro-eroded Ti6Al4V surface (D).

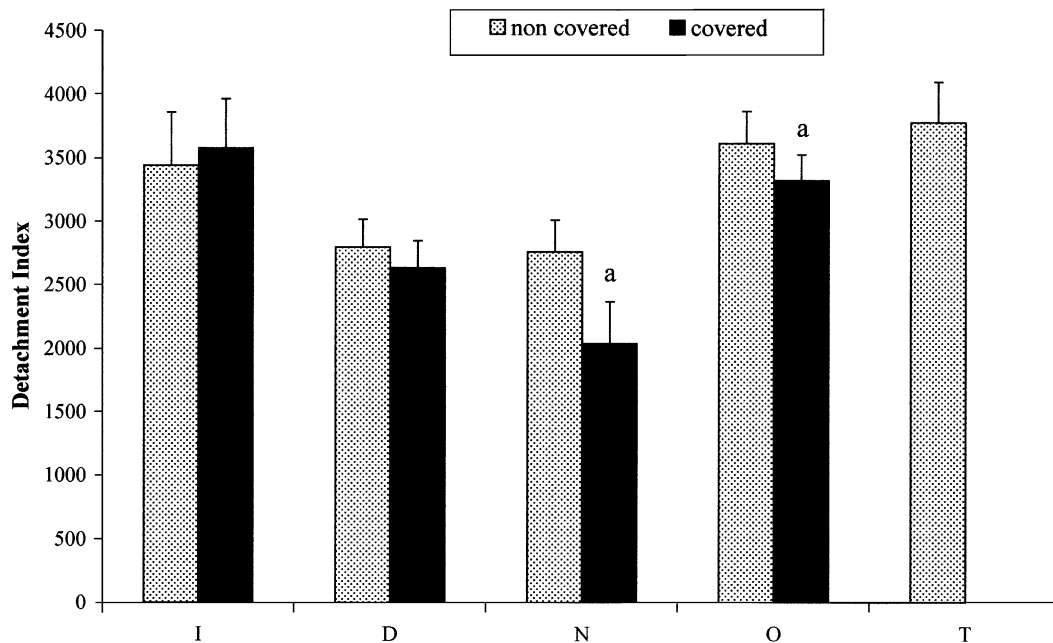


Fig. 12. Quantification of detachment index (DI) after 21 days of cells cultured on surfaces covered or non-covered by an Au-Pd layer. (I) polished Ti6Al4V surfaces, (D) fine electro-eroded Ti6Al4V surfaces, (N) fine electro-eroded titanium surfaces, (O) polished titanium surfaces and (T) Thermanox<sup>®</sup> cell culture treated plastic coverslips. Data indicate the mean + standard error ( $n = 6$ ). a—significantly different from non-covered surface at  $p \leq 0.05$ .

amplitude with a low level of organization above the cell scale (Order) and below the cell scale (Delta). At the macro-roughness level, we observe that hOB adhere and proliferate more on rough isotropic EE surfaces (C, D, M, N) > on rough anisotropic tool-machined surfaces (H) > smooth isotropic polished surfaces (I, MP, O) > smooth anisotropic tool-machined surfaces (A, B). From these observations, it appears that hOB adhere preferentially on rough surfaces at the scale

above the cell size. Observation at the micro-roughness level brings about the same results. However, at this scale, the H surfaces display discontinuities with a relatively low Rz and a high Delta, although the EE surfaces display discontinuities with a high Rz and a low Delta (Table 4). Moreover, analysis of the number of discontinuities (Peak) and the distance between them (SM) demonstrates that at the micro-roughness level EE surfaces have the lower number of discontinuities,

Table 4

|                 |       | Electro-eroded surfaces (C, D, M, N) | Coarse machine-tooled surfaces (H) | Controlled machine-tooled surfaces (A, B) | Polished surfaces (I, O, MP) |
|-----------------|-------|--------------------------------------|------------------------------------|---|------------------------------|
| Macro-roughness | Rz    | +++                                  | +++                                | ++  | +                            |
|                 | Order | +                                    | ++                                 | +++                                       | +++                          |
| Micro-roughness | Rz    | +++                                  | ++                                 | +   | +                            |
|                 | Delta | +                                    | +++                                | +++                                       | ++                           |
|                 | Peak  | +                                    | ++                                 | ++  | +++                          |
|                 | SM    | +++                                  | ++                                 | ++  | +                            |

separated by the larger space. From these observations we can conclude that CMS adhesion and proliferation is favoured by rough isotropic surfaces at the cellular scale although at the sub-cellular scale, they adhere preferentially on relatively smooth surfaces with few discontinuities. These observations are coherent with the bad CMS adhesion and proliferation results we obtained in our previous experiments on sandblasted surfaces, which had high Rz and high Delta and provided a substrate covered by a multitude of irregularities below the cell scale [14].

Additionally, on these isotropic EE surfaces, the cultured hOB present an original morphology close to the aspect of cells in vivo on human bone trabeculae [24]. This original cell morphology may be related to the 'smooth' topography of these surface below the cell scale and to the high roughness around the cells forming large, deep cavities with smooth slopes and banks providing 'nests' for cells.

## 5. Conclusion

In this experiment, the method we used to produce disordered surfaces, i.e. the electro-erosion process, appears to produce particularly favourable surfaces for in vitro hOB CMS adhesion and proliferation. For a complete description of their surface topography (amplitude and frequency roughness parameters) we attempted to understand the specificity of these EE surfaces. It appears that the main influential characteristics of these surfaces may be their isotropic aspect and the smooth aspect of the relief due to surface fusion during the process. When the topography is considered below the cell scale, cells appreciate their smooth surface although when the topography is considered above the cell scale, they appreciate a rough isotropic landscape formed by the numerous 'bowl-like nests' that favour their adhesion.

From the experiments described in this paper it appears that surface topography, rather than surface chemistry of the EE samples, influences the cell response. Although more complete investigations on

surface chemistry are needed to definitively conclude, we can consider that electro-erosion is a promising method for the preparation of bone implant surfaces. As this method could easily be applied to preparation of most biomaterials with complex geometries, further studies are needed for in vivo biocompatibility testing.

## Acknowledgements

This work was supported by the Fédération Biomatériaux Nord/Pas-de-Calais and by grants from the European Funds for Regional Development (FEDER) Obj.2-99.2-01b-n°78.

## References

- [1] Vercaigne S, Wolke JGC, Naert I, Jansen JA. Bone healing capacity of titanium plasma-sprayed and hydroxyapatite-coated oral implants. *Clin Oral Implant Res* 1998;9:261–71.
- [2] Suzuki K, Aoki K, Ohya K. Effects of surface roughness of titanium implants on bone remodeling activity of femur in rabbits. *Bone* 1997;21:507–14.
- [3] Klokkevold PR, Nishimura RD, Adachi M, Caputo A. Osseointegration enhanced by chemical etching of the titanium surface. *Clin Oral Implant Res* 1997;8:442–7.
- [4] Goldberg VM, Stevenson S, Feighan J, Davy D. Biology of grit-blasted titanium alloy implants. *Clin Ortho Relat Res* 1995; 319:122–9.
- [5] Vercaigne S, Wolke JGC, Naert I, Jansen JA. Histomorphometrical and mechanical evaluation of titanium plasma-sprayed-coated implants placed in the cortical bone of goats. *J Biomed Mater Res* 1998;41:41–8.
- [6] Feighan JE, Goldberg VM, Davy D, Parr JA, Stevenson S. The influence of surface-blasting on the incorporation of titanium-alloy implants in a rabbit intramedullary model. *J Bone Jt Surg* 1995;77-A:1380–95.
- [7] Bowers KT, Keller JC, Randolph BA, Wick DG, Michaels CM. Optimization of surface micromorphology for enhanced osteoblast responses in vitro. *Int J Oral Maxillofac Implants* 1992; 7:302–10.
- [8] Degasne I, Baslé MF, Demais V, Huré G, Lesourd M, Grolleau B, Mercier L, Chappard D. Effects of roughness, fibronectin and vitronectin on attachment spreading, and proliferation of human osteoblast-like cells (Saos-2) on titanium surfaces. *Calcif Tissue Int* 1999;64:499–507.

- [9] Cooper LF, Masuda T, Whitson SW, Yloheikkilä P, Felton DA. Formation of mineralizing osteoblast cultures on machined, titanium oxide grit-blasted, and plasma-sprayed titanium surfaces. *Int J Oral Maxillofac Implants* 1999;14:37–47.
- [10] Eisenbarth E, Meyle J, Nachtigall W, Breme J. Influence of the surface structure of titanium materials on the adhesion of fibroblasts. *Biomaterials* 1996;17:1399–403.
- [11] Castellani R, De Ruijter JE, Renggli H, Jansen JA. Response of rat bone marrow cells to differently roughened titanium discs. *Clin Oral Implant Res* 1999;10:369–78.
- [12] Links J, Boyan BD, Blanchard CR, Lohmann CH, Liu Y, Cochran DL, Dean DD, Schwartz Z. Response of MG63 osteoblast-like cells to titanium and titanium alloy is dependent on surface roughness and composition. *Biomaterials* 1998;19:2219–32.
- [13] Anselme K. Osteoblast adhesion on biomaterials. *Biomaterials* 2000;21:667–81.
- [14] Anselme K, Bigerelle M, Noel B, Dufresne E, Judas D, Iost A, Hardouin P. Qualitative and quantitative study of human osteoblast adhesion on materials with various surface roughness. *J Biomed Mater Res* 2000;49:155–66.
- [15] Anselme K, Noel B, Hardouin P. Human osteoblasts adhesion on titanium alloy, stainless steel, glass and plastic substrates with same surface topography. *J Mater Sci Mater Med* 1999;10:815–9.
- [16] Anselme K, Linez P, Bigerelle M, Le Maguer D, Le Maguer A, Hardouin P, Hildebrand HF, Iost A, Leroy J-M. The relative influence of the topography and chemistry of Ti6Al4V surfaces on osteoblastic cell behaviour. *Biomaterials* 2000;21:1567–77.
- [17] Lopez J, Hanseli G, Le Bosse JC, Mathia T. Caractérisation fractale de la rugosité tridimensionnelle de surface. *J Phys III* 1994;4:2501–19.
- [18] Larsson G, Thomsen P, Aronsson BO, Rodhal M, Lausmaa J, Kasemo B, Ericson LE. Bone response to surface-modified titanium implants: studies on the early tissue response to machined and electropolished implants with different oxide thicknesses. *Biomaterials* 1996;17:605–16.
- [19] Sun ZL, Wataha JC, Hanks CT. Effects of metal ions on osteoblast-like cell metabolism and differentiation. *J Biomed Mater Res* 1997;34:29–37.
- [20] Curtis A, Clark P. The effect of topographic and mechanical properties of materials on cell behavior. *CRC Rev. Biocompatibility* 1990;5:343–62.
- [21] Curtis A, Wilkinson C. Topographical control of cells. *Biomaterials* 1997;18:1573–83.
- [22] Den Braber ET, Jansen HV, de Boer MJ, Croes HJE, Elwenspoek M, Ginsel LA, Jansen JA. Scanning electron microscopic, transmission electron microscopic, and confocal laser scanning microscopic observation of fibroblasts cultured on microgrooved surfaces of bulk titanium substrata. *J Biomed Mater Res* 1998;40:425–33.
- [23] Walboomers XF, Croes HJE, Ginsel LA, Jansen JA. Growth behavior of fibroblasts on microgrooved polystyrene. *Biomaterials* 1998;19:1861–8.
- [24] Holtrop ME. The osteoblast and the osteocyte. In: Hall BK, editor. *Bone*. New Jersey, USA: The Telford Press Inc., 1990. p. 1–39.